Progress In Electromagnetics Research C, Vol. 37, 67–81, 2013

DESIGN OF PRINTED YAGI ANTENNA WITH ADDITIONAL DRIVEN ELEMENT FOR WLAN APPLICATIONS

Jafar R. Mohammed*

Communication Engineering Department, College of Electronic Engineering, University of Mosul, Mosul, Iraq

Abstract—A new configuration of Yagi antenna is proposed, which can improve the forward/backward ratio (f/b) significantly while maintaining a high gain. This configuration involves the addition of one radiating element to the original Yagi array. This additional element may arrange on parallel (side-by-side) or collinear to a radiating dipole of the original Yagi antenna. It is shown here that the technique is most effective for collinear configuration (exhibits smaller mutual effects) and that there then exists an optimum length and position for the added element. The amplitude of the excitation of the additional element determines the angular location of the back lobe reduction. To demonstrate the major benefits, comparisons are made among the proposed and conventional Yagi configurations. Numerical and measured results of our design show more than 20 dB front to back ratio at 2.4 GHz. Moreover, the proposed array represents a simple and valuable alternative to the stack Yagi antennas as the obtainable radiation characteristics are satisfactory in terms of both forward and backward gain.

1. INTRODUCTION

Most wireless local area network (WLAN) applications utilize omnidirectional antennas [1]. However, directional antennas such as printed Yagi arrays have been employed to suppress unwanted radio frequency emissions as well as unwanted interference in other directions. Yagi antennas have been utilized in industrial, scientific, and medical (ISM) applications at 2.4 GHz where directional radiation is necessary for long distance wireless communications and point-to-point communications. When designing Yagi antennas, the focus is

Received 12 December 2012, Accepted 28 January 2013, Scheduled 31 January 2013

* Corresponding author: Jafar Ramadhan Mohammed (jafarram@yahoo.com).

generally on compromising the performance of the gain, front-to-back (F/B) ratio and the bandwidth. In [2], it is demonstrated that, basically, none of these factors can be optimized without sacrificing the others.

There have been many printed Yagi antenna configurations that have been presented over the last 20 years [3–7]. The use of Yagi antenna designs in microstrip technology was first proposed by Huang in 1989 which consists of one reflector, one driven element, and two directors. These four patches are arranged on the same substrate surface in a way that the overall antenna characteristics are enhanced [3]. To increase the gain, Densmore and Huang introduced stacked Yagi antennas (each antenna consisting four elements) in four rows and excited the driven elements simultaneously [4]. This design can achieve a gain as high as 14 dBi, but F/B ratios around 4–5 dB may not be suitable for some applications. In [8, 9], a successful attempt to improve the F/B ratio of printed Yagi array antenna for WLAN and millimeter-wave applications was proposed. Additionally, in [10] a multiple-reflector structure is proposed to improve the F/B ratio of printed Yagi antennas without significantly sacrificing gain. However, the proposed design is suitable for planar array application.

In this paper, a design of printed Yagi antenna with one additional driven element is proposed to improve the radiation characteristics of the array in both forward and backward radiations. It is well-known that by increasing the length of the radiating dipole the radiation characteristics change and main beam becomes narrower. For proper dipole length, one could adjust the relative amplitude and phase of the excitation of the additional dipole to bring the main lobe of the additional dipole into alignment with the backside lobes of the original Yagi antenna pattern. Then, by subtracting the pattern of dipole antenna from that of the original Yagi array one could reduce the backside lobe in the radiation pattern of the original Yagi antenna.

Moreover, in some applications, such as interference from or to points off to one side or below the main lobe, the reduction in beam width is a more important consideration than the gain increase. In these applications, stacked Yagi antennas may be used to decrease the beamwidth [4, 9, 11]. However, unwanted large lobes may appear on each side of the main lobe with very low f/b ratio. These drawbacks can be overcome by the proposed antenna where beamwidth is reduced while maintaining a high f/b ratio with very low sidelobes level. This paper is organized as follows. Section 2 contains the principle of the proposed antenna configuration. Measurement and simulation results are illustrated in Section 3. Also in this section, the proposed Yagi antenna is applied over a frequency range from 2.3 GHz to 2.5 GHz to account for its potential use in WLAN applications. Finally, conclusions are given in Section 4.

2. PRINCIPAL OF THE PROPOSED ANTENNA

2.1. Antenna Configurations

The configurations of the proposed Yagi antenna with additional driven element are depicted in Figure 1. The additional driven element may be arranged on collinear (see Figure 1(a)) or parallel (see Figure 1(b)) with the radiating element of the original Yagi antenna. These configurations consists of original Yagi antenna to produce high gain

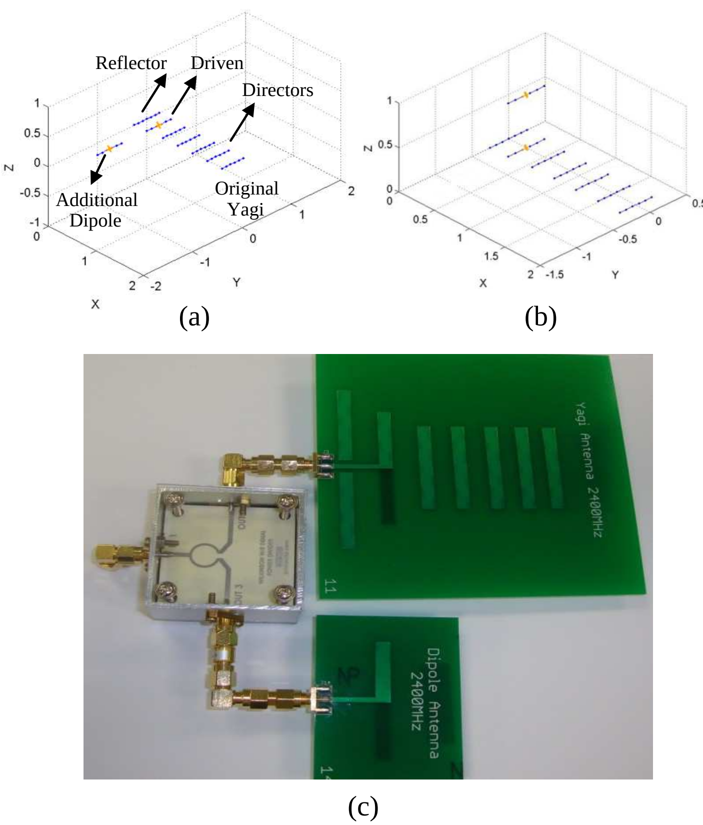

Figure 1. Proposed structures of the modified Yagi antenna. (a) Structure one. (b) Structure two. (c) Practical circuit for structure one.

radiation pattern toward desired direction, and an additional radiating dipole with phase shifter as well as attenuator to produce low gain adjustable radiation pattern that can be used to reduce the unwanted backside radiation of the original Yagi antenna.

It should be mentioned that the use of two additional radiating elements with linear array (all elements are radiating) for sidelobe cancellation was studied in [12]. However, the work presented in this paper involves the addition of one element only and the radiation characteristics can be controlled by changing its length. While the radiation characteristics in [12] was controlled by changing the separation distance between two additional elements. Furthermore, the measured results show that the technique of adding one radiating element is most effective for parasitic array like Yagi antenna.

2.1.1. Original Yagi Antenna

The Yagi antenna considered herein consists of K dipoles along the x-axes, namely, one reflector, one radiating dipole driven by a voltage generator, and the last $K-2$ being the directors. In order to compute the gain of the Yagi array, we assume that the currents are sinusoidal. The vector of voltage is:

$$\mathbf{V} = [0, 1, 0, 0, \ldots, 0]^T \tag{1}$$

Then, we compute the mutual impedance matrix $\mathbf{Z}$ and the input currents $\mathbf{I}$

$$\mathbf{I} = \mathbf{Z}^{-1}\mathbf{V} \tag{2}$$

Once we have the input currents $\mathbf{I} = [I_1, I_2, \ldots, I_K]^T$, the radiation intensity is given by [13]

$$U_{Yagi}(\theta, \varphi) = \frac{\eta}{8\pi^2}\left|\sum_{p=1}^{K} I_p \frac{\cos(kh_p\cos\theta) - \cos kh_p}{\sin kh_p \sin\theta}\, e^{jkx_p\sin\theta\cos\varphi}\right|^2 \tag{3}$$

Thus, the normalized gain of the array is computed by

$$G_{Yagi}(\theta, \varphi) = \left|\sum_{p=1}^{K} I_p \frac{\cos(kh_p\cos\theta) - \cos kh_p}{\sin kh_p \sin\theta} e^{jkx_p\sin\theta\cos\varphi}\right|^2 \tag{4}$$

where K is number of elements, $k = \frac{2\pi}{\lambda}$ the wave number, λ the wavelength, h_p the half-length of the pth element, and x_p the x-axis coordinates for $p = 1, 2, \ldots, K$.

Equations (2) and (4) provide a complete solution to the problem of coupled antenna arrays, based on the sinusoidal approximation for

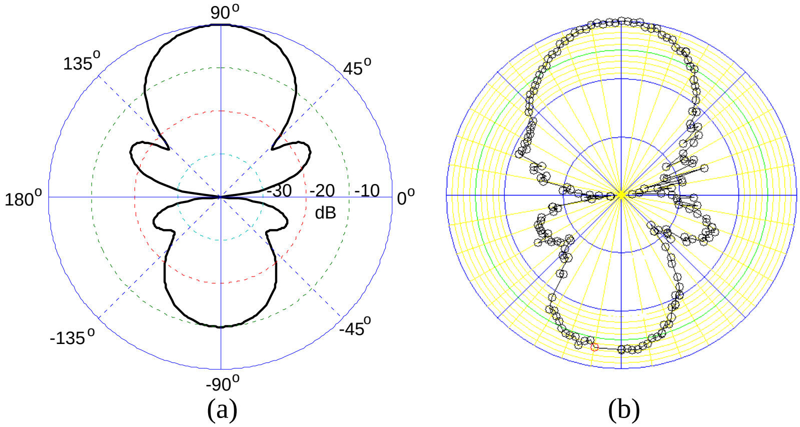

Figure 2. E-plane radiation patterns of original Yagi antenna. (a) Numerical result. (b) Measured result.

the currents. In the special case of identical antennas, Equation (4) factors into an array factor and an element factor:

$$G_{Yagi}(\theta,\varphi)=\left|\sum_{p=1}^{K} I_p e^{jkx_p\sin\theta\cos\varphi}\right|^2\left|\frac{\cos(kh\cos\theta)-\cos kh}{\sin kh\sin\theta}\right|^2 \tag{5}$$

Here the first factor represents the array factor while the second factor represents the element factor. The H-plane gain $G_H(\varphi)$ is defined to be the azimuthal gain on the xy-plane corresponding to $\theta=\pi/2$, and the E-plane gain $G_E(\theta)$ is defined to be the polar gain on any fixed azimuthal plane $\varphi=\varphi_o$. We assume that the lengths and spacing are such that the maximum gain is toward endfire, i.e., towards $\theta=90°$, $\varphi=0°$. The forward and backward gains are defined as:

$$G_f = G_{\max} = G(90°, 0) \tag{6}$$

$$G_b = G(90°, 180°) \tag{7}$$

Figure 2 presents calculated and measured radiation patterns (E-plane) of a seven-element equally spaced Yagi array. From these results there is good agreement between the measured and simulated radiation patterns. It is also observed that this antenna have a relatively large backward gain. By reducing the backward gain while maintaining high forward gain would be very useful for WLAN applications. The 3 dB beam width is approximately 44° for both measured and simulated patterns.

2.1.2. Dipole Antenna

For the dipole antenna, the radiation intensity can be written as

$$U_{dipole} = \eta \frac{|I_o|^2}{8\pi^2} \left[\frac{\cos\left(\frac{kl}{2}\cos\theta\right) - \cos\left(\frac{kl}{2}\right)}{\sin\theta} \right]^2 \tag{8}$$

The electric and magnetic field components of a dipole antenna can be written as [13]

$$E_\theta = j\eta \frac{I_o e^{-jkr}}{2\pi r} \left[\frac{\cos\left(\frac{kl}{2}\cos\theta\right) - \cos\left(\frac{kl}{2}\right)}{\sin\theta} \right] \tag{9}$$

$$H_\varphi = j \frac{I_o e^{-jkr}}{2\pi r} \left[\frac{\cos\left(\frac{kl}{2}\cos\theta\right) - \cos\left(\frac{kl}{2}\right)}{\sin\theta} \right] \tag{10}$$

where I_o constant, r is the radial distance and θ the polar angle. The normalized (to 0 dB) radiation pattern in E-plane of a half-wavelength dipole can be obtained from (8) by letting $l = \lambda/2$. Doing this, it reduce to

$$G_{(\lambda/2)\,dipole}(\theta) = \left[\frac{\cos\left(\frac{\pi}{2}\cos\theta\right)}{\sin\theta} \right]^2 \tag{11}$$

As can be seen from Equation (8) that the radiation intensity is a function of the length of the dipole (l). By varying l, its radiation

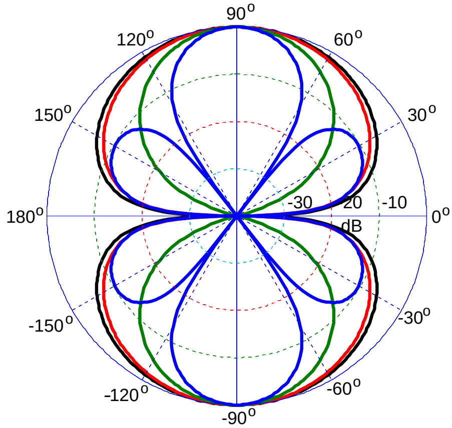

Figure 3. Radiation patterns for a thin dipole with sinusoidal current distribution ($l = \lambda/50$ (black color), $\lambda/2$ (red color), λ (green color), 1.25λ (blue color)).

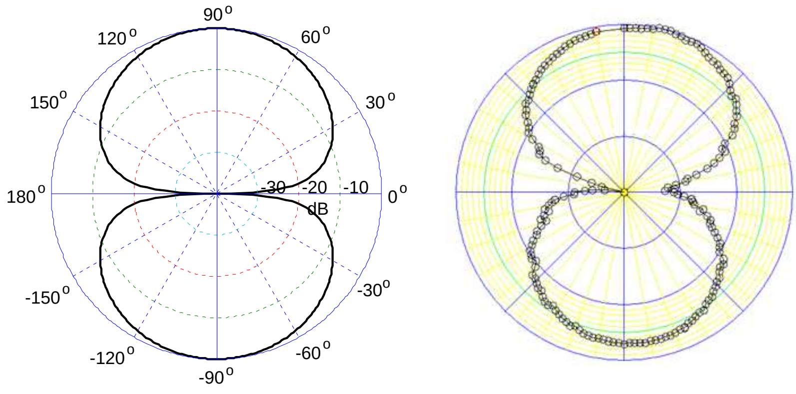

Figure 4. Radiation patterns of dipole antenna with length $l = 0.490\lambda$ (l = 5 cm) and at frequency 2.4 GHz. (a) Numerical result. (b) Measured result.

characteristics can be adjusted. The normalized radiation patterns, as given by (8) for $l = \lambda/50$, $\lambda/2$, λ, and 1.25λ are plotted in Figure 3. The radiation pattern for an infinitesimal dipole $l = \lambda/50$ is also included for comparison. It can be seen that as the length of the dipole antenna increases, the main beam becomes narrower. Because of that, the directivity should also increase with length. It is found that the 3 dB beamwidth of each is equal to

$$\begin{array}{ll} l \ll \lambda & 3\,\text{dB Beamwidth} = 90^\circ \\ l = \lambda/2 & 3\,\text{dB Beamwidth} = 78^\circ \\ l = \lambda & 3\,\text{dB Beamwidth} = 46^\circ \end{array}$$

As the length of the dipole antenna increases beyond one wavelength ($l > \lambda$), the number of lobes begin to increase. Figure 4 and Figure 5 show the measured radiation patterns of the dipole antenna at two different lengths $l = 0.490\lambda$ (l = 5 cm) and $l = 1.80\lambda$ (l = 24.4 cm) respectively. As illustrated in Figure 4 and Figure 5, the measured radiation pattern of a dipole becomes more directional as its length increases. When the overall length is greater than one wavelength, the number of lobes increases and the dipole antenna loses its directional properties. However, the main beam and the beam width of the dipole antenna are two of the important parameters that need to be considered in the proposed method (as will be discussed in the following section).

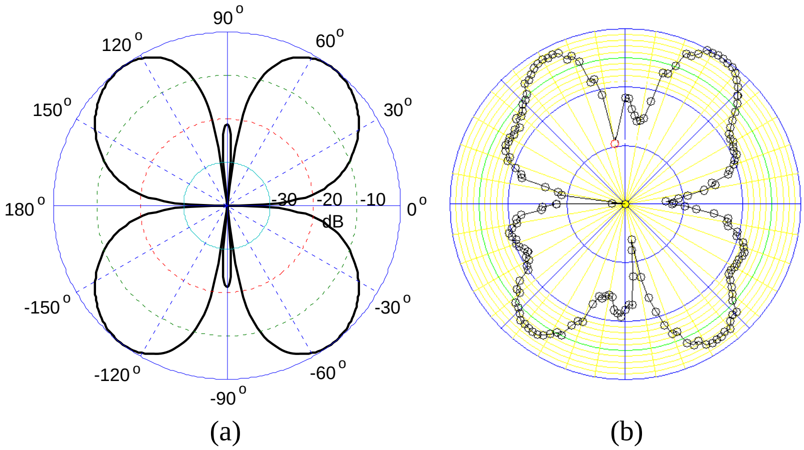

Figure 5. Radiation patterns of dipole antenna with length $l = 1.80\lambda$ ($l = 24.4\,\text{cm}$) and at frequency 2.4 GHz. (a) Numerical result. (b) Measured result.

2.2. Back Lobe Reduction

Consider the case where one radiating dipole is added to the Yagi array, as shown in Figure 1(c). Let the amplitude of its excitation be A and let the phase of its excitation be B. The total field radiated by the proposed antenna can be written,

$$E_T = \sum_{p=1}^{K} I_p e^{jkx_p \sin\theta\cos\varphi} \frac{\cos(kh_p\cos\theta) - \cos kh_p}{\sin kh_p \sin\theta} + Ae^{jB} \frac{\cos(\frac{kl}{2}\cos\theta) - \cos(\frac{kl}{2})}{\sin\theta} \tag{12}$$

We wish to set the values of amplitude and phase excitation for added dipole so as to achieve the objective of a sector of reduced backward radiation centered at angle ($\theta = -90°$ and $\varphi = 0°$). The approach is to properly set the length of dipole (l) and phase (B) so that the lobes of the radiation pattern of the dipole antenna are matched in width to the backside lobes of the original Yagi antenna and then to set the amplitude to cancel the backside lobes of the original Yagi antenna in the desired angular region. We choose the length of the added dipole to be equal to $l = 0.5\lambda$ which is equal to the length of the original driven element of the yagi antenna and the phase of the added dipole is chosen to be $B = \pi$ resulting in

$$E_T = \sum_{p=1}^{K} I_p e^{jkx_p \sin\theta\cos\varphi} \frac{\cos(\frac{\pi}{2}\cos\theta)}{\sin\theta} - A\frac{\cos(\frac{\pi}{2}\cos\theta)}{\sin\theta} \tag{13}$$

It is now quite obvious that the desired goal can be achieved by properly setting the value of amplitude excitation (A) of the added dipole; that is, setting

$$A = \sum_{p=1}^{K} I_p e^{jkx_p \sin(\theta_{backlobe})\cos(\varphi_{backlobe})} \tag{14}$$

Results in a total field

$$\begin{aligned} E_T = & \sum_{p=1}^{K} I_p e^{jkx_p \sin\theta\cos\varphi} \frac{\cos(\frac{\pi}{2}\cos\theta)}{\sin\theta} \\ & - \sum_{p=1}^{K} I_p e^{mathtijkx_p \sin(\theta_{backlobe})\cos(\varphi_{backlobe})} \frac{\cos(\frac{\pi}{2}\cos\theta)}{\sin\theta} \end{aligned} \tag{15}$$

which obviously has a zero at $\theta = \theta_{backlobe}$ and $\varphi = \varphi_{backlobe}$ (that is $\theta_{backlobe} = -90°$ and $\varphi_{backlobe} = 0°$). More importantly, however, it has a small magnitude in a wide region surrounding $\theta_{backlobe} = -90°$ by virtue of the matching of the back lobe widths discussed above.

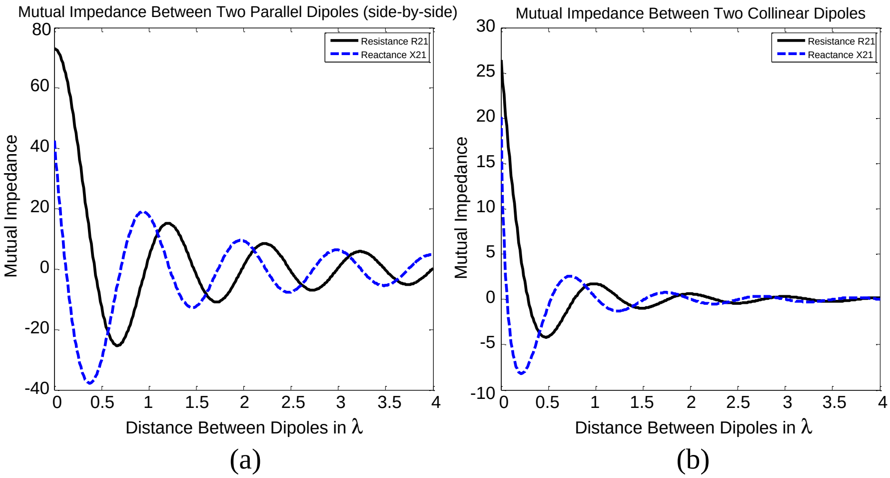

Figure 6. Mutual impedance of (a) two side-by-side and (b) collinear $\lambda/2$ dipoles using the induced EMF method.

This assumption is under the condition that the mutual effect between additional radiating dipole and original Yagi antenna is very small and may be neglected. To satisfy this requirement, first we need to study the effect of mutual coupling for two radiating dipoles that arranged either on parallel (side-by-side) or collinear [13]. The mutual impedance, referred to the current maximum, based on the induced emf method of a side-by-side and a collinear arrangement of two dipoles is shown plotted in Figure 6. It is apparent that the side-by-side arrangement exhibits larger mutual effects since the dipoles are placed in the direction of maximum radiation. To this aim, the collinear configuration is adopted in this paper. To further reduce the effect of mutual coupling, the separation distance between two antennas is chosen to be more than 1.0λ (see Figure 1(c)).

3. NUMERICAL AND MEASURED RESULTS

To illustrate the effectiveness of the proposed antenna configuration described above, we measured the radiation pattern for different design. The original Yagi antenna consists of seven dipoles (one reflector, one radiating dipole, and five directors) their lengths and x-locations were in units of λ

$$\begin{aligned}\mathbf{h} &= [h_1, h_2, h_3, h_4, h_5, h_6, h_7]\\ &= [0.510\lambda, 0.490\lambda, 0.430\lambda, 0.430\lambda, 0.430\lambda, 0.430\lambda, 0.430\lambda]\\ \mathbf{x} &= [x_1, x_2, x_3, x_4, x_5, x_6, x_7]\\ &= [-0.25\lambda, 0, 0.310\lambda, 0.620\lambda, 0.930\lambda, 1.24\lambda, 1.55\lambda]\end{aligned}$$

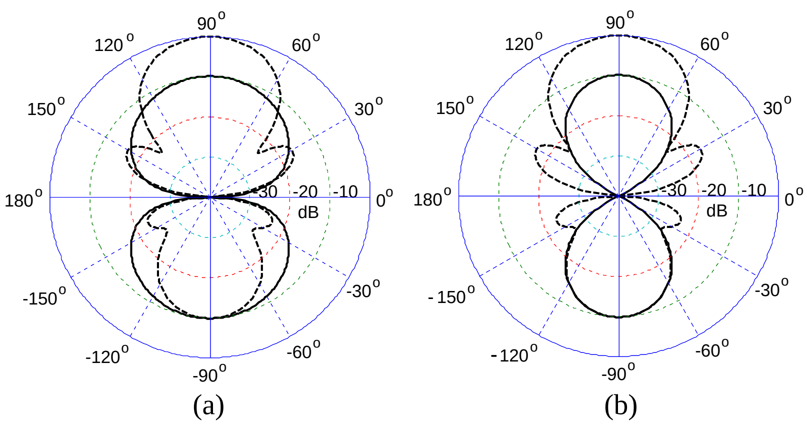

Figure 7. Radiation patterns of original Yagi antenna (dotted line) and dipole antenna (solid line) for different l. (a) Numerical result for $l = 0.490\lambda$. (b) Numerical result for $l = 1.0\lambda$.

The proper values of the phase and amplitude excitation of the additional dipole are set by using 180 phase shifter and -10 dB attenuator. We begin with the case of $l = 0.490\lambda$ (or $l = 5$ cm), i.e., the length of the additional dipole is equal to the length of radiating dipole of the original Yagi antenna. The matching between beam widths of the original Yagi and added dipole is illustrated in Figure 7(a). For this case, the resulting pattern is shown in Figure 8. Note the reduction in the backward radiation. It is also apparent from Figure 7(b) that the best matching between these two aforementioned radiation patterns are occurs when we choose the length of dipole antenna $l = 1.0\lambda$ (or $l = 12.4$ cm). The simulated and measured results for this case are shown in Figure 9. Note that the reduction in the backside radiation is extended over wide region centered at -90°. Note also the 3 dB beamwidth is reduced from 44° in original Yagi to 38° in the proposed antenna. The gain of the original Yagi antenna was 11.9 dB, while the gain of the proposed antenna was 11.7 dB. The front-to-back ratio at 2.4 GHz is higher than 20 dB and is much higher than previous woks [8–10].

Note also that the measured patterns that were shown in Figures 8(b) and 9(b) differ slightly from the calculated patterns that are shown in Figures 8(a) and 8(b) especially at the center of the back lobes (i.e., around $\theta = -90^\circ$ and $\varphi = 0^\circ$). This asymmetry of the back lobes caused by the asymmetry of the measurement environments. The measurement of the radiation patterns are made in a normal room

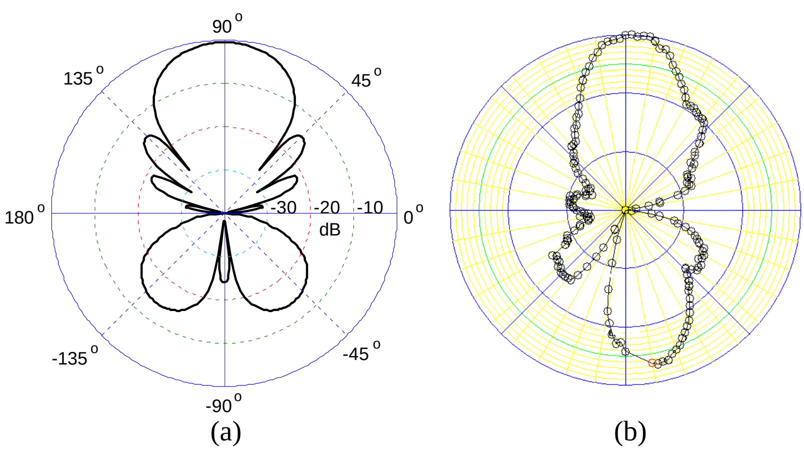

Figure 8. Radiation patterns of dipole antenna with length $l = 0.490\lambda$ ($l = 5$ cm) and at frequency 2.4 GHz. (a) Numerical result. (b) Measured result.

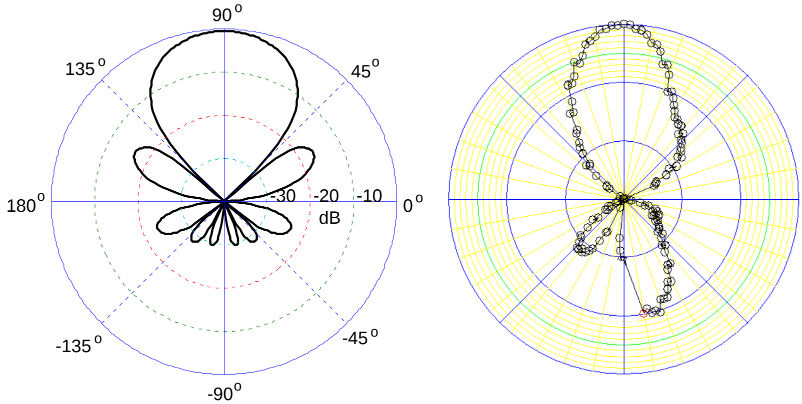

(a) (b)

Figure 9. Radiation patterns of dipole antenna with length $l = 1.0\lambda$ ($l = 12.4\,\mathrm{cm}$) and at frequency 2.4 GHz. (a) Numerical result. (b) Measured result.

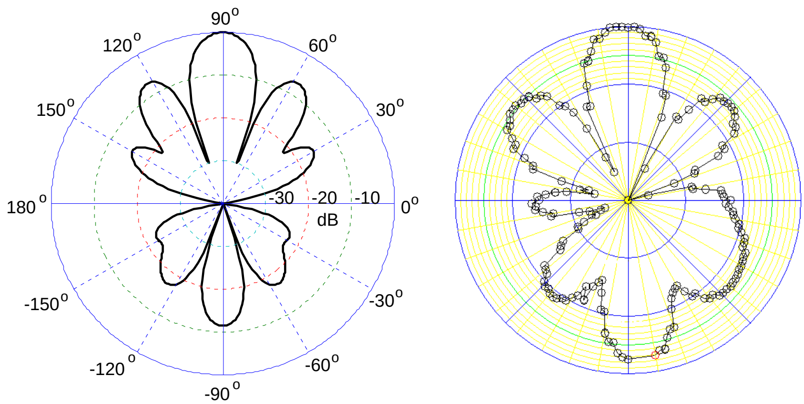

(a) (b)

Figure 10. Radiation patterns of two stack Yagi antennas (collinear). (a) Numerical result. (b) Measured Result.

(i.e., it includes some structures such as computers, tables, … etc.). Therefore, some differs exist in the measured results.

To demonstrate the major benefits, a performance comparison of the proposed configuration and stacked Yagi antennas [4, 9] is provided. In this case, two printed Yagi antennas were combined (each Yagi consisting seven elements). For the purpose of fair comparison,

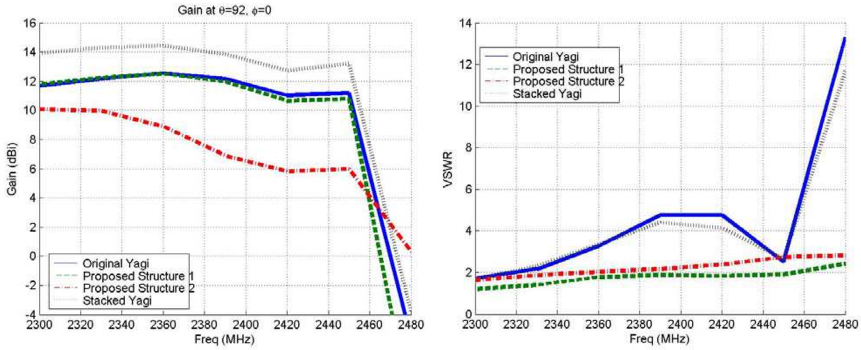

Figure 11. The gain and VSWR as a function of frequency for the original Yagi, proposed structures, and stacked two Yagi antennas.

the separation distance between two Yagi antennas was kept same as the distance between the added dipole and original Yagi in the proposed antenna. Also, collinear arrangement of these two stacked Yagi antennas was used The simulation and measured results for these two stacked Yagi antennas are shown in Figure 10. It can be seen that the large lobes have appeared on each side of the main lobe and 6 dB down. Although, the gain is increased about 1.6 dB but at the cost of high radiation in the unwanted directions and this may not be suitable for some applications

Finally, the original Yagi, proposed antennas (structure 1 and structure 2), and stacked two Yagi antennas were simulated over a frequency range from 2.3 GHz to 2.5 GHz to account for their bandwidth. The carrier frequency was set equal to 2.4 GHz in all antennas. The gain and VSWR versus frequency are depicted in Figure 11. Note that the good performance of the structure one ($\text{VSWR} \leq 1.9$ and gain > 11 dBi) is maintained over a frequency range from 2.3 GHz up to 2.45 GHz. Note also the gain of the stacked two Yagi antennas was increased about 1.6 dB in most frequency range. However, it have values of $\text{VSWR} > 5$ at 2.4 GHz.

4. CONCLUSION

In this paper, the design of the Yagi antenna with an additional radiating dipole has been presented for WLAN applications. The radiation characteristics of the proposed array in both forward and backward radiation were significantly improved. The additional dipole is arranged on collinear to the radiating dipole of the original Yagi antenna. In comparison to an original Yagi antenna, measurement of the proposed antenna has improvement in F/B ratio more than 15 dB at 2.4 GHz

Moreover, the proposed antenna was compared to well-designed two stacked Yagi antennas (each Yagi has seven elements). These two Yagi antennas were aligned on collinear with separation distance about 6 cm. The gain was increased about 1.6 dB but at the cost of larger sidelobes and backward radiation. On the other hand, the proposed antenna can simultaneously achieve high gain with a very low radiation in back lobe and side lobes directions.

The principal of the new antenna array may be extended to various types of antennas.

REFERENCES

1. Wu, Y., B. Sun, J. Li, and Q. Liu, "Triple-band omni-directional antenna for WLAN application," *Progress In Electromagnetics Research*, Vol. 76, 477–484, 2007.
2. Pozar, D., "Microstrip antennas," *Proc. IEEE*, Vol. 80, No. 1, 79–91, Jan. 1992.
3. Huang, J., "Planar microstrip Yagi array antenna," *IEEE Antennas and Propagation Society Int. Symp.*, Vol. 2, 894–897, Jun. 1989.
4. Densmore, A. and J. Huang, "Microstrip Yagi antenna for mobile satellite vehicle application," *IEEE Trans. Antennas Propag.*, Vol. 39, No. 7, 1024–1030, Jul. 1991.
5. Xin, Q., F.-S. Zhang, B.-H. Sun, Y.-L. Zou, and Q.-Z. Liu, "Dual-band Yagi-Uda antenna for wireless communications," *Progress In Electromagnetics Research Letters*, Vol. 16, 119–129, 2010.
6. Lin, S., G.-L. Huang, R.-N. Cai, and J.-X. Wang, "Novel printed Yagi-Uda antenna with high-gain and broadband," *Progress In Electromagnetics Research Letters*, Vol. 20, 107–117, 2011.
7. Ta, S. X., H. Choo, and I. Park, "Wideband double-dipole Yagi-Uda antenna fed by a microstrip-slot coplanar stripline transition," *Progress In Electromagnetics Research B*, Vol. 44, 71–87, 2012.
8. DeJean, G. R. and M. M. Tentzeris, "A new high-gain microstrip Yagi array antenna with a high front-to-back (F/B) ratio for WLAN and millimeter-wave applications," *IEEE Trans. Antennas Propag.*, Vol. 55, No. 2, 298–304, Feb. 2007.
9. Bemani, M. and S. Nikmehr, "A novel wide-band microstrip

Yagi-Uda array antenna for WLAN applications," *Progress In Electromagnetics Research B*, Vol. 16, 389–406, 2009.

10. Huang, E. and T. Chiu, "Printed Yagi antenna with multiple reflectors," *Electronics Letters*, Vol. 40, No. 19, Sep. 16, 2004.
11. Khodier, M. and M. Al-Aqil, "Design and optimization of Yagi-Uda antenna arrays," *IET Microw. Antennas Propag.*, Vol. 4, No. 4, 426–436, Apr. 2010.
12. Mohammed, J. R., "A new technique for obtaining wide-angular nulling in the sum and difference patterns of monopulse antenna," *IEEE Antennas and Wireless Propagation Letters*, Vol. 11, 1242–1245, 2012.
13. Balanis, C. A., *Antenna Theory: Analysis and Design,* 3rd Edition, John Wiley & Sons, Hoboken, New Jersey, 2005.